Neonatal fibrin scaffolds promote enhanced cell adhesion, migration, and wound healing *in vivo* compared to adult fibrin scaffolds

Kimberly Nellenbach[1,2], Seema Nandi[1,2], Christopher Peeler[1], Alexander Kyu[1], Ashley C. Brown[1,2*]

[1]Joint Department of Biomedical Engineering, North Carolina State University and The University of North Carolina at Chapel Hill, Raleigh, NC 27695

[2]Comparative Medicine Institute, North Carolina State University, Raleigh, NC 27695

Abstract

Introduction: Fibrin scaffolds are often utilized to treat chronic wounds. The monomer fibrinogen used to create such scaffolds is typically derived from adult human or porcine plasma. However, our previous studies have identified extensive differences in fibrin network properties between adults and neonates, including higher fiber alignment in neonatal networks. Wound healing outcomes have been linked to fibrin matrix structure, including fiber alignment, which can affect the binding and migration of cells. We hypothesized that fibrin scaffolds derived from neonatal fibrin would enhance wound healing outcomes compared to adult fibrin scaffolds.

Methods: Fibrin scaffolds were formed from purified adult or neonatal fibrinogen and thrombin then structural analysis was conducted via confocal microscopy. Human neonatal dermal fibroblast attachment, migration, and morphology on fibrin scaffolds were assessed. A murine full thickness injury model was used to compare healing *in vivo* in the presence of neonatal fibrin, adult fibrin, or saline.

Results: Distinct fibrin architectures were observed between adult and neonatal scaffolds. Significantly higher fibroblast attachment and migration was observed on neonatal scaffolds compared to adults. Cell morphology on neonatal scaffolds exhibited higher spreading compared to adult scaffolds. *In vivo* significantly smaller wound areas and greater epidermal thickness were observed when wounds were treated with neonatal fibrin compared to adult fibrin or a saline control.

Conclusions: Distinctions in neonatal and adult fibrin scaffold properties influence cellular behavior and wound healing. These studies indicate that fibrin scaffolds sourced from neonatal plasma could improve healing outcomes compared to scaffolds sourced from adult plasma.

AUTHOR BIOGRAPHY

Dr. Brown received a B.S. from Clemson University in Biosystems Engineering in 2006 and a Ph.D. from Georgia Tech in Bioengineering in 2011. Dr. Brown performed her postdoctoral studies in the School of Chemistry and Biochemistry and the Wallace H. Coulter Department of Biomedical Engineering at Georgia Tech and she was an American Heart Association (AHA) Postdoctoral Fellow. Dr. Brown joined the Joint Department of Biomedical Engineering at North Carolina State University and the University of North Carolina at Chapel Hill as an Assistant Professor in 2015. Her research focuses on developing novel soft materials for a variety of

biomedical applications including augmentation of hemostasis, enhanced wound healing, evaluation and modulation of cellular mechanotransduction and development of biosynthetic constructs for regenerative medicine. Dr. Brown's research is supported by the NIH, NSF, and AHA. Dr. Brown is actively involved in several national societies including the American Society for Matrix Biology (ASMB), Society for Biomaterials (SFB), and Biomedical Engineering Society (BMES); she currently serves as a Council Member for ASMB and SFB and is Co-Chair of the BMES Student Affairs Committee. Dr. Brown is also an NSF CAREER Award recipient.

Key Terms: fibrin scaffold, neonate, wound healing, regenerative medicine, hydrogels

Introduction:

In the United States, approximately 6.5 million patients are affected by chronic, non-healing wounds[3,13]. Upon the onset of an injury, enzymatic action of thrombin on the plasma protein fibrinogen leads to formation of a crosslinked fibrin network[36]. This matrix provides a provisional scaffold for infiltrating cells that support tissue repair and angiogenesis[7]. A deficient provisional fibrin matrix can result in non-healing wounds. Accelerating the wound healing process is crucial for non-healing wounds to avoid complications such as infection[15]. Fibrin sealants are a topical therapeutic that have been developed to aid in hemostasis and promote wound closure. They primarily consist of plasma-derived fibrinogen and thrombin and act to mimic the final stages of the coagulation cascade; the formation of a stable fibrin network that facilitates wound healing. Fibrin sealants are an attractive class of biomaterials due to their biodegradable and biocompatible nature[28]. However, their formulations require reagent concentrations (i.e. fibrinogen and thrombin) well above physiological ranges and result in fibrin matrices that are much denser than native clots[28]. These thick, dense fibrin networks have much lower porosity than networks comprised of physiologically relevant concentrations of fibrinogen and thrombin, and can impede cell migration and inhibit matrix degradation, resulting in slower wound healing rates[28]. The monomer fibrinogen used to create such scaffolds is typically derived from adult human or porcine plasma[17]. However, our previous studies have identified extensive differences in fibrin network properties between adults and neonates, including higher fiber alignment in neonatal networks[4]. Wound healing outcomes have been linked to fibrin matrix structure, including fiber alignment, which can affect the binding and migration of cells. We hypothesized that fibrin scaffolds derived from neonatal fibrin would enhance wound healing outcomes compared to adult fibrin scaffolds. Here, we

investigate the use of a novel fibrin scaffold derived from neonatal fibrinogen, as opposed to adult fibrinogen, to enhance wound healing outcomes.

In recent years, extensive differences have been identified in fibrinogen and fibrin network properties between adults and neonates (infants less than 30 days of age)[4,15]. Although neonates and adults have similar levels of plasma fibrinogen, neonates have decreased clotting activity and an increased clotting time.[15] At the protein level, neonatal fibrinogen has been found to have increased sialic acid and phosphorus content compared to the mature form[1,15,32]. Differences have also been identified at the bulk fibrin clot level. Clots formed from purified neonatal or adult fibrinogen displayed significantly different structural and functional characteristics. Specifically, purified neonatal fibrin clots appeared more porous and highly aligned when compared to the denser, branched networks seen in adult networks. Functionally, purified neonatal fibrin networks have significantly faster rates of matrix degradation compared to adults[4]. Additionally, recent studies from our group using atomic force microscopy (AFM) to obtain elastic moduli of platelet poor plasma (PPP) clots indicate neonatal clots are significantly softer than adult clots[25]. These age-dependent differences in fibrinogen and fibrin clot properties have also been identified in porcine samples[25]. However, the impact of these age-dependent fibrin network discrepancies on cell behavior have not been previously explored.

The effectiveness of wound healing has been linked to fibrin matrix properties, including structural and mechanical characteristics. Structurally, the porosity and density of fibrin networks have been shown to influence cellular binding and migration and subsequent tissue growth[21]. Additionally, functional qualities including mechanical and fibrinolytic properties have also been shown to influence migration and proliferation of cells[6]. Here, we performed a comparative study of cellular behavior and wound healing outcomes on neonatal fibrin matrices compared to adult.

The previously identified differential fibrin network properties in neonates could impact cell behavior and subsequent wound healing outcomes. These age-dependent differences may also be a factor in fetal scarless wound healing, a phenomenon in which in utero wounds heal through complete regeneration, rather than repair[20]. We hypothesized that fibrin scaffolds produced from neonatal fibrin would promote enhanced cell migration and wound healing outcomes compared to adult fibrin due to inherent biochemical and structural differences. The objective of this research was to determine if differences exist in cell behavior and wound healing outcomes on neonatal fibrin scaffolds compared to traditional fibrin scaffolds derived from adult fibrin.

Methods:

Isolation of fibrinogen from platelet poor plasma:

Neonatal and adult human fibrinogen was isolated from plasma samples via ethanol precipitation reaction[26]. After IRB approval from Emory University and informed written parental consent, whole blood samples were collected from human neonates (less than 30 days of age) undergoing elective cardiac surgery at the Children's Hospital of Atlanta. 5 mL of whole blood was collected from an arterial line placed after the induction of anesthesia and prior to surgical incision. Samples were centrifuged immediately to yield PPP and stored at -80 until use. Pooled adult human PPP was obtained from the New York Blood Center and stored at -80 until use. Pooled plasma samples were then utilized for isolation of either adult or neonatal fibrinogen. Ethanol (70% volume) was added to 4°C plasma in a 4:1 ratio (plasma/ethanol) and cooled on ice for 20 minutes. The solution was centrifuged at 600 g for 15 minutes at 4°C. The supernatant was then removed, and the resulting pellet is heated in a 37°C water bath. A buffer consisting of 20 mM sodium citrate was added until the pellet was completely dissolved (0.25-0.5 mL). This method mainly selectively precipitates fibrinogen, however, trace amounts of other plasma proteins including Von

Willebrand Factor, plasminogen, and fibronectin may be present[10,16].If necessary, fibrinogen solution was concentrated using Pall Nanosep centrifugal devices (Pall, Port Washington, NY, USA). Concentration of samples was determined using a Nano-drop (Thermofisher Scientific, Waltham, MA,USA). For all *in vitro* assays, conditions were run with a minimum of two separate isolated fibrinogen batches. *For in vivo* studies, a single isolation batch was used.

Structural characterization of fibrin matrices:

Structural analysis of fibrin clots was conducted with confocal microscopy. 50 μl clots consisting of purified adult or neonatal fibrinogen at a concentration of 2.5 mg/mL in HEPES buffer (5 mM calcium, 7.4 pH) were formed with the addition of 0.5 U/mL human α-thrombin. 10 μg/mL Alexa 488 labeled fibrinogen was used for visualization. Clots were formed between a glass slide and coverslip and allowed to polymerize for two hours prior to imaging. A Zeiss Laser Scanning Microscope (LSM 710, Zeiss Inc., USA) at a magnification of 63x was utilized for imaging and a minimum of three random z-stacks of 5.06 μm thickness were acquired per clot. ImageJ software was used to create 3D projections from z-stacks. Fiber alignment was quantified through a MATLAB algorithm previously utilized by our group[4]. The code can be found at https://github.com/Kanellen/Fiber-alignment. Briefly, each confocal microscopy image was preprocessed by padding with redundant data and applying a gaussian decay and two dimensional Hann window to minimize edge effects prior to application of a two-dimensional Fast Fourier transform. The resulting power spectrum was utilized to determine alignment by polar coordinate analysis and relative intensity of pixels in angular bins. The alignment index (AI) was determined from the fraction of fibers aligned within +/- 20 degrees of a preferred fiber alignment normalized to random distribution of oriented fibers (equal to 40°/180°). Alignment index values range from 1.0 to 4.55. Alignment analysis was conducted for each image in the z-stack and averaged together.

Clot fiber density was determined from the ratio of black (fiber) over white (background) pixels in each image. Fibrin network branching was quantified with a custom MATLAB code. Briefly, a multiscale-hessian filtering method was applied to each image slice to identify tubular structures. Structure sensitivity was determined through a threshold based on the intensity distribution. The image was than binarized and skeletonized. Fiber overlap was then quantified from the skeletonized image by reducing intersections of fibers to single points. These branch points were normalized across the area of the image and averaged across each stack. Each image of the three-dimensional stack was processed individually and then averaged together.

Removal of sialic acid from fibrinogen:

To determine the influence of sialic acid on neonatal and adult fibrin structure, sialic acid was cleaved from neonatal and adult fibrinogen via neuraminidase®. A 500 µl fibrinogen solution consisting of 5 mg/mL adult or neonatal fibrinogen in diH_2O was incubated with 0.025 U Neuraminidase (Neuraminidase/Sialidase, Sigma Aldrich, USA) for 4 hours at 35°C. Removal of bound sialic acid was confirmed by determining the concentration of sialic acid in the fibrinogen solution before and after enzyme digestion (Sialic Acid (NANA) Assay Kit, Abcam, USA). The solution was centrifuged and stored at -80°C until use in confocal microscopy experiments.

Cell attachment on fibrin matrices:

Cell attachment on fibrin matrices was analyzed via a florescence based assay. Neonatal and adult fibrin networks (2.5 mg/mL) were formed with 0.5 U/mL human α-thrombin (Enzyme Research Laboratories, South Bend, IN, USA) in a 96-well plate and polymerized for 2 hours. Neonatal human dermal fibroblasts (HDFn) (Gibco, Waltham, MA, USA) (P5-P14) were fluorescently labeled (Vybrant Dii, Thermofisher Scientific, Waltham, MA, USA) according to manufacture instructions, seeded on top of fully polymerized fibrin gels, and incubated for 1 hour at 37°C.

After 1 hour, three washes with PBS were performed to remove non-adherent cells and florescence intensity (Abs:549 nm, Em: 565 nm) was determined via plate reader (Biotek Synergy H1). It is possible that fluorescence intensity may vary from cell to cell, therefore, cell attachment was also quantified from confocal microscopy images taken at 40x from cells seeded at a density of 12,000 cells/well and fixed after 16 hours. Cell count was determined as the number of cells in the field of view. The average values from 12 images at the same magnification are reported.

Cell spreading on fibrin:

Cell spreading on fibrin films was analyzed via confocal microscopy. Uniform fibrin films were formed on coverslips using modified standardized protocols[30]. To create hydrophilic bottom coverslips to adhere to fibrin matrices, a 0.1 M sodium hydroxide (NaOH) solution was added to coverslips in a 12 well cell culture plate and left to evaporate. The coverslips were then functionalized with (3-Aminopropyl)triethoxysilane (APTMS) for 5 minutes at room temperature. Once dry, a 0.05% glutaraldehyde solution was added to each well and left to incubate for 30 minutes followed by 3 washes with H_2O. Neonatal and adult fibrin gels consisting of 2.5 mg/mL fibrinogen and 0.5 U/mL human α-thrombin were then formed on functionalized coverslips and immediately covered with dichlorodimethylsilane (DCDMS) coated coverslips. After 2 hours of polymerization, top coverslips were removed and fibrin gels were stored at 4°C until use. Gels were sterilized via UV light for 30 mins prior to cell attachment. HDFns were seeded on fibrin gels at a density of 12,000 or 6,000 cells per well and media (HDFn growth medium; DMEM, 10% fetal bovine serum, 1% pencillin-streptomycin, 1% L-glutamine); up to 1 mL was added to each well. Plates were then incubated for 16 hours at 37°C. Cells were fixed with 4% paraformaldehyde in PBS and stained with Alexa 488 labeled phalloidin for visualization. Samples were mounted with Vectashield with Dapi (Fisher Scientific, Hampton, NH, USA) to visualize nuclei and

coverslips were sealed with nail polish. Confocal microscopy (Zeiss LSM 710) was utilized to examine cell morphology and cell area, perimeter, and circularity were calculated with ImageJ.

Evaluation of in vitro cell migration in neonatal vs. adult fibrin matrices

HDFns were cultured into spheroids over 72 hours using a hanging drop cell culture technique[5]. Fibrin clots composed of 2.5 mg/ml human neonatal or fibrinogen and 0.5 U/ml human α-thrombin (Enzyme Research Laboratories, South Bend, IN, USA) were created in the wells of a 96-well tissue culture plate (VWR, Radnor, PA, USA). After a 2 hour polymerization period, cell spheroids were transferred onto a fibrin clot using a 21 G x 1 ½' needle (BD Biosciences, San Jose, CA, USA) and then covered with a second fibrin layer to create a 3D environment. After a 2 hour polymerization time for the second fibrin layer, HDFn growth medium (DMEM, 10% fetal bovine serum, 1% penicillin-streptomycin, 1% L-glutamine) was added into each well, and spheroids were imaged every 24 hours for a 72-hour period. Cell migration throughout the fibrin matrix was quantified by measuring the projected spheroid surface area for each 2D image using ImageJ.

Evaluation of wound healing in vivo

Wound healing *in vivo* in the presence of neonatal and adult fibrin scaffolds was assessed using a murine wound healing model previously described by Dunn *et al*[11]. All protocols were approved by the NCSU IACUC prior to conducting studies. 8 week old C57/B6 mice (Charles River Laboratories, Wilmington, MA, USA) were anesthetized with 5% isoflurane in oxygen in an induction box prior to surgery. Throughout the duration of the surgery, general anesthesia was maintained with a nosecone at 3% isoflurane. Full thickness dermal wounds were created using 4 mm biopsy punches (Fisher Scientific, Hampton, NH, USA) and splinted with 10 mm silicone rings with a 5mm inner diameter. Wounds were splinted to force healing through reepithelization rather than skin contraction as it is more physiologically relevant to humans. 10 μL of neonatal or

adult fibrin scaffold treatments created with 2.5 mg/mL fibrinogen polymerized in the presence of 0.5 U/mL human α-thrombin were applied topically with 0.9% sterile filtered saline as a control group (n = 6 wounds/group). Wounds were imaged and covered with Opsite bandages (Fisher Scientific, Hampton, NH, USA). Carprofen (ApexBio, Houston, TX, USA) (5 mg/kg) was administered subcutaneously for pain relief for the first five days post-surgery. Wounds were imaged and dressings were changed every day for nine days post-surgery. Wound size analysis was performed on wound images that were blinded by treatment group and randomized using a random number generator. Wound sizes were quantified using ImageJ and normalized to the silicone ring openings. Normalized wound areas were used to determine wound closure rates for each treatment group. Total wound healing rate was calculated as the total percent wound closure on day 9 divided by 9.

Animals were euthanized under carbon dioxide and then tissue surrounding the wounds was excised nine days post-surgery and fixed in 10% formalin. Tissue samples were ethanol dehydrated, embedded in paraffin wax, and sectioned for analysis. Martius Scarlet Blue (MSB) staining was performed to identify collagen and fibrin within the wound site. Epidermal thickness was quantified from MSB images by measuring the thickness of the epidermal layer at 3 regions across the wound area. CD31 labeling was performed to evaluate angiogenesis within tissue forming at the wound sites. Tissue was deparaffinized, rehydrated, and incubated with 1% goat serum (Thermo Fisher Scientific, Waltham, MA, USA). Sections were labeled with a rabbit anti-mouse monoclonal antibody to CD31 (1:50, clone SP38, Thermo Fisher Scientific, Waltham, MA, USA) overnight at 4°C. Sections were then washed in PBS and labeled with Alexa 594 goat anti-rabbit as a secondary antibody for one hour at room temperature. Sections were then washed in PBS and mounted with Vectashield HardSet mounting medium with DAPI (Fisher Scientific,

Hampton, NH, USA). CD31 positively labeled tissue was quantified via previously published protocols[23,29]. Briefly, ImageJ Particle Analysis was used to measure total red area (defined as red area greater than 1.0 μm^2 with a threshold of 0-50) in wounds.

Statistical Analysis:

Statistical analysis was performed in GraphPad Prism 7 (GraphPad, San Diego, CA, USA). Data was analyzed via a One-way Analysis of Variance (ANOVA) with a Tukey's post hoc test using a 95% confidence interval for all measurements except for analysis of wound closure, which was conducted with a two way ANOVA. Outlier tests were performed prior to all statistical analysis. No outliers were found and no data was removed. Data is presented as average +/- standard deviation.

Results:

Structural characterization of fibrin matrices:

Fibrin matrix architecture has been shown to influence fibroblast infiltration and migration[21]. Therefore, we hypothesized that the differences observed in adult and neonatal fibrin scaffolds would likewise differentially influence fibroblast behavior. Here, we utilized confocal microscopy to compare the architecture of fibrin scaffolds constructed from neonatal or adult fibrin (**Figure 1A**). At equal fibrinogen (2.5mg/mL) and thrombin (0.5 U/mL) concentrations we observed major structural distinctions between clots that are consistent with patterns identified in our previous studies[4,24]. Specifically, adult fibrin networks were found to have a dense, branched structure compared to the highly porous, low cross branching structure seen in neonatal networks. Analysis of fiber density using the ratio of black to white pixels revealed significantly lower fiber density in neonatal samples compared to adult scaffolds (**Figure 1B**) (Neonatal fibrin: 0.684 +/- 0.157, Adult fibrin: 1.350 +/- 0.201, $p<0.0001$). Using a custom MATLAB code for fiber alignment we

observed a higher, although not statistically significant, degree of fiber alignment in the neonatal samples compared to adult (**Figure 1C)** (Neonatal fibrin: 1.095 +/- 0.073 alignment index, Adult fibrin: 1.054 +/- 0.030 alignment index, p=0.142). Quantification of fibrin branching indicated significantly more branch points per area in adult samples compared to neonate (**Figure 1D)** (Neonatal fibrin: 0.045 +/- 0.006 branch points/ μm^2, Adult fibrin: 0.057 +/- 0.010 branch points /μm^2, $p<0.01$).

Cells display enhanced attachment, spreading, and migration on neonatal fibrin scaffolds:

Fibroblast attachment to the provisional fibrin matrix is a crucial step in wound healing and is mediated by surface integrin $\alpha v\beta 3$[12]. Fibrin architecture is known to influence fibroblast attachment, spreading, and migration, therefore we hypothesized that the differences observed in adult and neonatal fibrin scaffolds would likewise differentially influence fibroblast behavior. To that end, fibroblast attachment on neonatal or adult fibrin scaffold was first explored with fluorescently labeled fibroblasts (**Figure 2**). After the 1 hour incubation period, attachment of fibroblasts on neonatal fibrin matrices was found to be significantly higher than on adult fibrin (Neonatal fibrin: 0.647 +/- 0.027 fluorescence intensity, Adult fibrin: 0.594 +/- 0.026 fluorescence intensity, $p<0.01$). Additionally, cell attachment was determined from cell counts on images taken after 16 hours of incubation (**Supplemental Figure 1**). Similarly, cell attachment on neonatal fibrin matrices was higher than on adult fibrin matrices in these experiments (Neonatal fibrin: 42.91 +/- 24.92 cells/field of view, Adult fibrin: 26.00 +/- 13.21 cells/field of view, $p<0.05$). While the underlying specific cause of structural differences between neonatal and adult fibrin networks remains a topic of investigation and is likely multifactorial, these differences could be due to differences in posttranslational modifications. Previous studies have identified differences in sialic content between adult and neonatal fibrinogen[15], therefore, we next investigated the

influence of sialic acid on the observed cell attachment responses by removing sialic acid from the fibrinogen prior to fibrin polymerization and then evaluated cell attachment. When sialic acid was removed from both adult and neonatal fibrinogen with neuraminidase incubation, no significant differences in fibroblast attachment were observed on fibrin scaffolds, indicating the presence of sialic acid may influence cell attachment (**Figure 3**) (Neonatal fibrin: 0.466 +/- 0.064 fluorescence intensity, Adult fibrin: 0.455 +/- 0.056 fluorescence intensity). We next characterized cell morphology of adherent fibroblasts on neonatal and adult fibrin scaffolds with confocal microscopy at 6,000 cells/well **(Figure 4)** and 12,000 cells/well (**Supplemental Figure 2).** At various cell densities, cell area and perimeter were increased with decreased cell circularity on neonatal fibrin scaffolds compared to fibroblast parameters on adult fibrin matrices (6,000 cells/well; cell area; Neonatal fibrin: 1571.09 +/- 397.82 μm^2 Adult fibrin: 877.12 +/- 323.02 μm^2, $p<0.0001$, cell perimeter: Neonatal fibrin: 311.99 +/- 73.95 μm, Adult fibrin: 184.94 +/- 55.45 μm, $p<0.0001$, cell circularity; Neonatal fibrin: 0.223 +/- 0.09 , Adult fibrin: 0.4138 +/- 0.11, $p<0.0001$). Finally, we evaluated fibroblast migration through 3D neonatal or adult fibrin scaffolds using a spheroid based assay. Fibroblast migration through fibrin networks was observed over a 72 hour period (**Figure 5**). Cell migration was found to be significantly greater at 48 and 72 hours on neonatal derived fibrin scaffolds compared to adult (48 hours: Neonatal fibrin: 248.16 +/- 63.29 % change from day 0, Adult fibrin: 27.75 +/- 18.27 % change from day 0, $p<0.0001$, 72 hours: Neonatal fibrin: 425.61 +/- 107.89 % change from day 0, Adult fibrin: 38.57 +/-11.68 % change from day 0, $p<0.0001$).

Evaluation of wound healing in vivo

Fibroblasts migrate into the provisional fibrin matrix and synthesize new extracellular matrix during native wound healing to form new tissue[21]. Based on our results demonstrating enhanced

cell attachment and migration on neonatal fibrin scaffolds compared to adult scaffolds, we hypothesized that wound healing outcomes would also be improved. To assess this, neonatal or adult fibrin clots (2.5 mg/mL fibrinogen, 0.5 U/mL thrombin) or a saline control were applied to full thickness dermal wounds in adult mice. Rates of wound closure was assessed by measuring the wound area over the 9 day period. Evaluation of wound closure indicated an overall greater rate of closure and significantly smaller wound areas on day 9 in mice treated with neonatal fibrin compared to adult fibrin and saline treatment groups (wound closure rate; Neonatal fibrin: 5.21 +/- 1.91% closure/day, Adult fibrin: 3.628 +/- 1.605% closure/day, Saline 2.72 +/- 0.987% closure/day, Neonatal fibrin vs. Saline $p<0.05$) (**Figure 6)**. Histological analysis of wound tissue stained with MSB staining revealed a more robust epithelial layer with significantly greater thickness in neonatal fibrin treated wounds compared to wounds from mice treated with a saline control (Neonatal fibrin: 48.33 +/-20.84 μm, Adult Fibrin: 35.67 +/- 15.03 μm, Saline: 21.27 +/- 13.86 μm. Neonatal fibrin vs. Saline $p<0.05$) (**Figure 7**). Immunohistochemistry staining for angiogenic marker CD31 indicated increased angiogenesis in wounds treated with neonatal fibrin relative to wounds treated with adult fibrin or saline, although statistical significance was not reached (Neonatal fibrin: 23630.00 +/- 35634.40 μm^2, Adult Fibrin: 5040.5 +/- 4057.33 μm^2, Saline: 1744 +/- 2687.34 μm^2).

Discussion and Conclusions:

In these studies, we demonstrate that neonatal fibrin network properties differentially influence cell behavior compared to scaffolds comprised of adult fibrin. Fibroblast attachment, spreading, and migration was greater on neonatal derived fibrin scaffolds. Additionally, the topical application of neonatal fibrin to full thickness dermal wounds enhanced wound closure *in vivo*. These studies demonstrate that neonatal fibrin properties positively direct cell behavior resulting

in enhanced wound healing outcomes, indicating that fibrin scaffolds sourced from neonatal plasma could improve healing outcomes compared to scaffolds sourced from adult plasma.

While the differences in cell responses and wound healing outcomes on neonatal fibrin scaffolds compared to adult fibrin scaffolds are likely multifactorial, structural differences may play a role. Structural characterization revealed significant age-dependent differences in matrix organization at equal thrombin concentrations. Neonatal scaffolds were more aligned and less dense than adult scaffolds, consistent with trends identified in our previous studies[4,24,25]. These distinct structural architectures have been previously linked to differences in fibrin network degradation and may influence additional clot mechanical properties[31]. Importantly, previous studies have linked scaffold structural properties to cell behavior[21,35]. Increased matrix porosity, which is dependent on the thickness and density of the fibrin fibers, is linked to increased cellular infiltration and tissue growth[8]. With lower fiber and intersection density, neonatal fibrin networks have a higher permeability to allow for increased cell penetration and migration throughout the scaffold. Fibrinogen naturally contains two common arginine-glycine-aspartic acid (RGD) binding motifs to facilitate in cell adhesion[27]. Research has shown that cell attachment can be directed by topological cues from substrate microenvironment including physical and biochemical properties[2]. At equal starting cell densities and incubation times, significantly greater fibroblast attachment was observed on neonatal fibrin networks compared to adult networks. Because more aligned fibers promote cell migration to a greater degree than randomly aligned fibers, the aligned structure of the neonatal networks likely also contributes to the enhanced cell migration through these scaffolds[35,37].

While the underlying specific cause of these structural differences remains unclear and future studies exploring fibrin polymerization mechanisms in neonates is necessary to fully

understand these structural patterns, our results demonstrate that increased sialic acid content of neonatal fibrinogen may play a role. Previous research has indicated that neonatal fibrinogen has biochemical differences compared to the mature adult form, including increased sialic acid content which contributes to an overall more negative protein charge[1]. Hyper-salinated fibrinogen has also been identified in patients with liver disease and is characterized by an increased negative charge, altered matrix structure, and delayed fibrin clotting times, which is speculated to be caused by increased electrostatic repulsion between fibers[19,33]. To determine if the differential sialic acid content affects cell attachment patterns, fibroblast attachment was evaluated on neonatal and adult fibrin matrices with sialic acid removed via neuraminidase digestion. When sialic acid was removed via enzymatic digestion, fibroblast attachment was no longer significantly different between adult and neonatal fibrin matrices, indicating the increased glycosylation contributes to the higher fibroblast attachment seen with normal neonatal fibrin. The impact on attachment may be due to effects related to the increased negative charge from the sialic acid or steric availability of RGD binding sites but future studies are needed to determine the underlying mechanism. Since sialic acid content does play a role in cell attachment behavior, it is possible that sialyation of adult fibrinogen may result in fibrin network properties that recapitulate those of neonatal fibrin. Future studies exploring fibrin matrix properties, cell behavior, and wound healing outcomes on hypersialyinated adult fibrinogen are necessary to determine the potential as a protein source for biomaterial development.

Fibroblast morphology and migration has also been shown to be dependent upon underlying matrix organization[2,35,37]. Confocal microscopy analysis of HDfn morphology revealed significantly greater cell area and decreased fibroblast circularity on neonatal fibrin networks compared to adult. Additionally, we observed a higher degree of fibroblast alignment on neonatal

fibrin matrices compared to adult. Cells have been shown to align and elongate longitudinally on cylindrical substrates as is observed on different tissue types across physiological systems[37]. With our observed lower cross branching density and greater concentrations of longitudinal fiber organization in neonatal scaffolds, elongation of fibroblasts along longitudinal fiber axes most likely contribute to decreased circularity. Next, we quantified cell migration by embedding fibroblast spheroids within a neonatal or adult fibrin network and analyzing migration over 72 hours. Our results indicated significantly greater fibroblast migration away from spheroid bodies when embedded in neonatal fibrin networks compared to adult. This may be due to the increased fibrin matrix porosity seen in neonatal fibrin networks that allows for greater cell infiltration into the scaffold. Additionally, recent studies have also indicated that 3D fibroblast migration is facilitated in softer fibrin matrices and previous research from our group has shown that neonatal plasma clots are significantly less stiff than adult[22,24]. Therefore, this mechanical aspect is likely a contributing factor to cell infiltration rates. As mentioned above, increased fiber alignment in neonatal scaffolds is also a potential contributing factor to increased migration.

Enhanced fibroblast migration has been linked to acceleration of healing of excisional wounds[23]. With our findings of enhanced fibroblast migration through neonatal scaffolds, we hypothesized that we would observe enhanced healing in wounds treated with neonatal fibrin. Indeed, topical application of neonatal fibrin to full thickness excisional wounds in mice resulted in significantly smaller wound areas nine days post injury compared to mice treated with adult fibrin or saline. In histological analysis of wounds nine days post injury, we observed formation of significantly thicker epidermal layers in wounds treated with neonatal fibrin relative to those treated with saline, indicating more robust healing and epidermal regeneration. Immunolabeling for CD31+ revealed greater angiogenesis in wounds treated with neonatal fibrin, although

statistical significance was not reached, most likely due to the large variances between these samples. Overall would healing outcomes were greater in animals treated with neonatal fibrin compared to adult fibrin or saline controls.

The primary goal of this research was to characterize the effects of neonatal vs. adult fibrin on cell behavior and wound healing outcomes. Overall, these studies indicate that the biochemical and structural differences between neonatal and adult fibrin scaffolds affect fibroblast attachment, spreading, and migration and ultimately lead to enhanced dermal wound healing outcomes. Improved wound healing has been previously identified in neonatal animals where incisional dermal wounds healed faster and free of fibrotic responses, following fetal-like wound repair patterns, compared to adult counterparts[34]. Much of the work to recapitulate this enhanced wound healing has been focused on the diversity and quantities of cytokine expression during wound healing. Here, we show that the properties of the provisional fibrin matrix affect cell patterns and subsequent wound healing results. Biochemical contributions from increased sialic acid content of neonatal fibrinogen were shown to directly impact cell attachment. Structural matrix properties including fibrin density most likely also contribute to the differential cell and wound healing outcomes between neonatal and adult fibrin groups. The results of these studies are applicable to the development of novel fibrin-based scaffolds to accelerate wound repair in patients with chronic wounds. However, this study has several limitations. We indicated that the distinct mechanical properties between neonatal and adult fibrin scaffolds may influence cell behavior. In our previous experiments obtaining the elastic moduli of PPP clots under compressive forces, bulk scaffold stiffness was lower in neonatal derived groups compared to adult groups. However, the alignment of fibers in neonatal clots may increase stiffness in the direction parallel to fibers due to mechanical anisotropy. Further studies are needed to characterize mechanical anisotropy. Also, in our

experiments, we utilized adult derived human thrombin to form fibrin scaffolds. In order to investigate age-dependent differences in fibrin, this reagent source and concentration was kept consistent. To date, no significant differences have been described between neonatal and adult thrombin except lower generation in neonates[14]. However, this should be considered in future studies. Additionally, in our experiments analyzing cell morphology on fibrin scaffolds, glass surfaces were functionalized to create uniform fibrin films. It is possible that this process of tethering the fibrin to the surface could alter fibrin properties and/or affect cellular responses. The minimum clot volume utilized in these experiments was 30 μL, resulting in scaffolds at least 10 μm thick. Research has indicated that cell-soft matric interactions can be significantly altered by an underlying substrate at 2-3 μm in thickness[6]. Therefore, the cells in these experiments are most likely responding to the fibrin scaffold not the underlying glass. However, there is the possibility that tethering the fibrin to the glass could affect cell mechanotransduction. If so, we expect equal effects between adult and neonatal groups.

There are also important considerations for our *in vivo* wound healing model utilized in this study. In order to properly recapitulate human wound healing, dermal wounds were splinted, which requires a longer duration under anesthesia and creates the potential of local inflammation at suture sites. Nonetheless, this splinting is crucial to promote wound healing through re-epithelialization, cell proliferation, and angiogenesis, which more closely resembles healing patterns in humans[11]. Finally, while sourcing neonatal plasma from human donors is certainly not feasible ethically or practically, recently, we identified similar age-dependent patterns in fibrinogen and fibrin clot properties in pigs[25]. Neonatal porcine and human fibrin clots had closely matched structural, mechanical, and fibrinolytic characteristics[25]. Porcine sources are frequently used for clinically used fibrin based hemostatic materials, therefore, for future use in biomaterial

development, porcine plasma could be utilized as a neonatal fibrinogen source, thereby increasing the translational potential of this work.

In summary, the results of this research determined that distinctions in neonatal and adult fibrin clot properties influence cellular behavior and wound healing. Cell attachment, migration, and spreading was greater on neonatal fibrin films and led to greater wound healing outcomes. The results of this research are critical for the understanding of age dependent differences in wound healing and the development of therapeutic technologies for treatment of chronic wounds. In particular, fibrin scaffolds sourced from neonatal porcine plasma could improve healing outcomes compared to scaffolds sourced from adult plasma.

Acknowledgements: Funding for this project was provide by start-up funds for Ashley Brown from North Carolina State University, DMR-1847488 from the National Science Foundation, and CDMRP W81XWH-15-1-0485 from the U.S. Department of Defense. The authors would like to thank Eva Johannes, PhD, Director at the Cellular and Molecular Imaging Facility at North Carolina State University for technical assistance with microscopy, Nina Guzzetta, M.D. from Children's Healthcare of Atlanta and Emory University for providing neonatal plasma samples, and Lucas Timmins, PhD from University of Utah for assistance with Matlab code.

Conflicts of interest: Kimberly Nellenbach, Seema Nandi, Christopher Peeler, Alexander Kyu, and Ashley C. Brown declare that they have no conflicts of interest.

Ethical standards: All human subjects research was carried out in accordance with Department of Health and Human Services policy and regulations and approved by the Emory University IRB. All animal studies were carried out in accordance with North Carolina State University policies and regulations including meeting standards and guidelines set forth by the NIH Guide for the Care

and Use of Laboratory Animals. All animal studies were approved by the North Carolina State University IACUC.

Work Cited:

1. Andrew, M., L. Mitchell, L.R. Berry, B. Schmidt, and M.W.C. Hatton. Fibrinogen Has a Rapid Turnover in the Healthy Newborn Lamb. *Pediatr. Res.* 23:249–252, 1988.

2. Baker, B.M., and C.S. Chen. Deconstructing the third dimension – how 3D culture microenvironments alter cellular cues. *J. Cell Sci.* 125:3015–3024, 2012.

3. Bitsch, M. *et al.* Epidemiology of chronic wound patients and relation to serum levels of mannan-binding lectin. *Acta Derm. Venereol.* 89:607–611, 2009.

4. Brown, A.C., R. Hannan, L.H. Timmins, J.D. Fernandez, T.H. Barker, and N.A. Guzzetta. Fibrin network changes in neonates after cardiopulmonary bypass. *Anesthesiology* 124:1021–1031, 2016.

5. Brown, L.F., N. Lanir, J. McDonagh, K. Tognazzi, A.M. Dvorak, and H.F. Dvorak. Fibroblast migration in fibrin gel matrices. *Am. J. Pathol.* 142:273–283, 1993.

6. Buxboim, A., K. Rajagopal, A.E.X. Brown, and D.E. Discher. How deeply cells feel: methods for thin gels. *J. Phys. Condens. Matter Inst. Phys. J.* 22, 2010.

7. Chester, D., and A.C. Brown. The role of biophysical properties of provisional matrix proteins in wound repair. *Matrix Biol.* 60–61:124–140, 2017.

8. Chiu, C.L., V. Hecht, H. Duong, B. Wu, and B. Tawil. Permeability of Three-Dimensional Fibrin Constructs Corresponds to Fibrinogen and Thrombin Concentrations. *BioResearch Open Access* 1:34–40, 2012.

9. Diaz-Mauriño, T., C. Castro, and A. Albert. Desialylation of fibrinogen with neuraminidase. Kinetic and clotting studies. *Thromb. Res.* 27:397–403, 1982.

10. Dietrich, M. *et al.* Fibrin-Based Tissue Engineering: Comparison of Different Methods of Autologous Fibrinogen Isolation. *Tissue Eng. Part C Methods* 19:216-226, 2012.

11. Dunn, L., H.C.G. Prosser, J.T.M. Tan, L.Z. Vanags, M.K.C. Ng, and C.A. Bursill. Murine Model of Wound Healing. *J. Vis. Exp. JoVE* , 2013 [cited 2020 Jan 14]. Available from: https://www.ncbi.nlm.nih.gov/pmc/articles/PMC3724564/.

12. Gailit, J., C. Clarke, D. Newman, M.G. Tonnesen, M.W. Mosesson, and R.A. Clark. Human fibroblasts bind directly to fibrinogen at RGD sites through integrin alpha(v)beta3. *Exp. Cell Res.* 232:118–126, 1997.

13. Gottrup, F. Optimizing wound treatment through health care structuring and professional education. *Wound Repair Regen. Off. Publ. Wound Heal. Soc. Eur. Tissue Repair Soc.* 12:129–133, 2004.

14. Haidl, H. *et al.* New insights into neonatal coagulation: normal clot formation despite lower intra-clot thrombin levels. *Pediatr.* 86:719-724, 2019.

15. Ignjatovic, V., A. Ilhan, and P. Monagle. Evidence for age-related differences in human fibrinogen. *Blood Coagul. Fibrinolysis Int. J. Haemost. Thromb.* 22:110–117, 2011.

16. Ismail, A.E. Purification of Fibrinogen from Human Plasma. [Lincoln, Nebraska]: University of Nebraska, , 2012. Available from: https://digitalcommons.unl.edu/cgi/viewcontent.cgi?article=1012&context=chemengtheses.

17. Jackson, M.R. Fibrin sealants in surgical practice: An overview. *Am. J. Surg.* 182:1S-7S, 2001.

18. Järbrink, K. *et al.* Prevalence and incidence of chronic wounds and related complications: a protocol for a systematic review. *Syst. Rev.* 5:152, 2016.

19. Langer, B.G., J.W. Weisel, P.A. Dinauer, C. Nagaswami, and W.R. Bell. Deglycosylation of fibrinogen accelerates polymerization and increases lateral aggregation of fibrin fibers. *J. Biol. Chem.* 263:15056–15063, 1988.

20. Larson, B.J., M.T. Longaker, and H.P. Lorenz. Scarless Fetal Wound Healing: A Basic Science Review. *Plast. Reconstr. Surg.* 126:1172–1180, 2010.

21. Laurens, N., P. Koolwijk, and M.P.M. de Maat. Fibrin structure and wound healing. *J. Thromb. Haemost. JTH* 4:932–939, 2006.

22. Leon-Valdivieso, C.Y. *et al.* Fibroblast migration correlates with matrix softness. A study in knob-hole engineered fibrin. *APL Bioeng.* 2:036102, 2018.

23. Nandi, S. *et al.* Platelet-like particles dynamically stiffen fibrin matrices and improve wound healing outcomes. *Biomater. Sci.* 7:669–682, 2019.

24. Nellenbach, K., N.A. Guzzetta, and A.C. Brown. Analysis of the structural and mechanical effects of procoagulant agents on neonatal fibrin networks following cardiopulmonary bypass. *J. Thromb. Haemost. JTH* 16:2159–2167, 2018.

25. Nellenbach, K.A., S. Nandi, A. Kyu, S. Sivadanam, N.A. Guzzetta, and A.C. Brown. Comparison of Neonatal and Adult Fibrin Clot Properties between Porcine and Human Plasma. *Anesthesiol. J. Am. Soc. Anesthesiol.* , 2020.Available from: https://anesthesiology.pubs.asahq.org/article.aspx?articleid=2760520.

26. Qiu, L.L., S.S. Levinson, K.L. Keeling, and R.J. Elin. Convenient and effective method for removing fibrinogen from serum specimens before protein electrophoresis. *Clin. Chem.* 49:868–872, 2003.

27. Salsmann, A., E. Schaffner-Reckinger, F. Kabile, S. Plançon, and N. Kieffer. A New Functional Role of the Fibrinogen RGD Motif as the Molecular Switch That Selectively Triggers Integrin αIIbβ3-dependent RhoA Activation during Cell Spreading. *J. Biol. Chem.* 280:33610–33619, 2005.

28. Spotnitz, W.D. Fibrin Sealant: The Only Approved Hemostat, Sealant, and Adhesive—a Laboratory and Clinical Perspective. *ISRN Surg.* 2014, 2014. Available from: https://www.ncbi.nlm.nih.gov/pmc/articles/PMC3960746/.

29. Sproul, E.P., S. Nandi, C. Roosa, L. Schreck, and A.C. Brown. Biomimetic Microgels with Controllable Deformability Improve Healing Outcomes. *Adv. Biosyst.* 2:1800042, 2018.

30. Tse, J.R., and A.J. Engler. Preparation of hydrogel substrates with tunable mechanical properties. *Curr. Protoc. Cell Biol.* Chapter 10:Unit 10.16, 2010.

31. Undas, A., and R.A.S. Ariëns. Fibrin clot structure and function: a role in the pathophysiology of arterial and venous thromboembolic diseases. *Arterioscler. Thromb. Vasc. Biol.* 31:e88-99, 2011.

32. Van Cott, E.M., E.Y. Smith, and D.K. Galanakis. Elevated Fibrinogen in an Acute Phase Reaction Prolongs the Reptilase Time but Typically Not the Thrombin Time. *Am. J. Clin. Pathol.* 118:263–268, 2002.

33. Varki, A. Sialic acids in human health and disease. *Trends Mol. Med.* 14:351–360, 2008.

34. Wagner, W., and M. Wehrmann. Differential cytokine activity and morphology during wound healing in the neonatal and adult rat skin. *J. Cell. Mol. Med.* 11:1342-1352, 2007.

35. Wang, W.Y. *et al.* Extracellular matrix alignment dictates the organization of focal adhesions and directs uniaxial cell migration. *APL Bioeng.* 2:046107, 2018.

36. Weisel, J.W., and R.I. Litvinov. Mechanisms of fibrin polymerization and clinical implications. *Blood* 121:1712–1719, 2013.

37. Werner, M., A. Petersen, N.A. Kurniawan, and C.V.C. Bouten. Cell Migration: Cell-Perceived Substrate Curvature Dynamically Coordinates the Direction, Speed, and Persistence of Stromal Cell Migration. *Adv. Biosyst.* 3:1970102, 2019.

Figures:

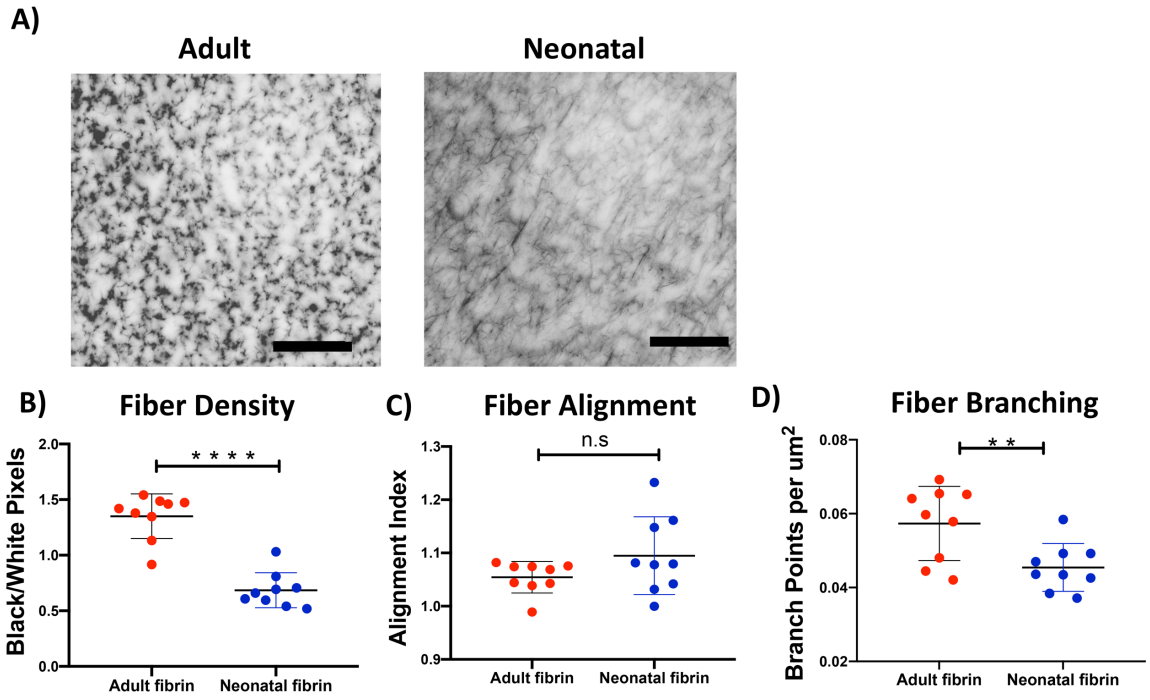

Figure 1: Neonatal and adult fibrin scaffolds are structurally distinct. (A) Representative confocal images taken at 63x of adult or neonatal fibrin clots polymerized with 2.5 mg/mL fibrinogen and 0.5 U/mL thrombin. (B) Fiber density was calculated as the ratio of black (fibers) over white (space) fibers. (C) Alignment index and (D) quantification of branch points was conducted with custom MATLAB codes. N=3 clots per group with 3 random images each. Mean +/- standard deviation is shown. Scale = 10 μm. p**<0.01, p***<0.001.

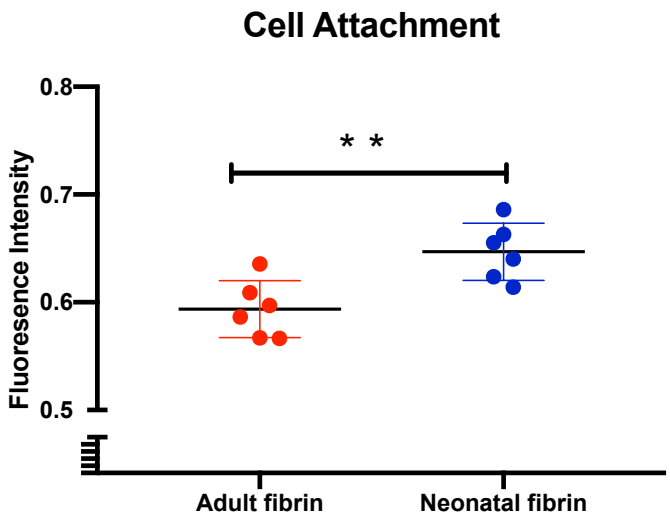

Figure 2. Fibroblast attachment is greater on neonatal fibrin scaffolds. Fluorescently labeled HDFns were seeded on adult or neonatal derived fibrin scaffolds and attachment was investigated after 1 hour via fluorescent plate reader. Mean attachment +/- standard deviation is shown. N=6 wells per group. p**<0.01.

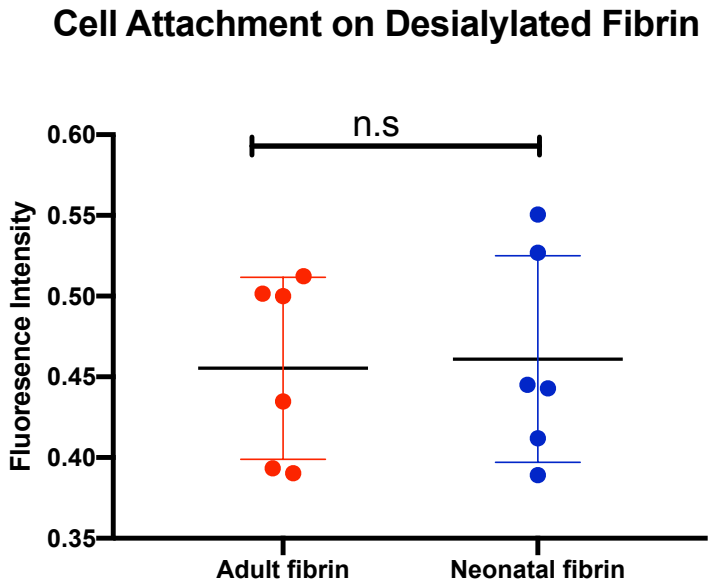

Figure 3. Fibroblast attachment is similar on desalinated adult and neonatal fibrin scaffolds. Sialic acid was cleaved via neuraminidase digestion and then fibroblast attachment on desalinated fibrin scaffolds was investigated. Fluorescently labeled HDFns were seeded on adult or neonatal derived desalinated fibrin scaffolds and attachment was investigated after 1 hour via fluorescent plate reader. Mean attachment +/- standard deviation is shown. N=6 wells per group.

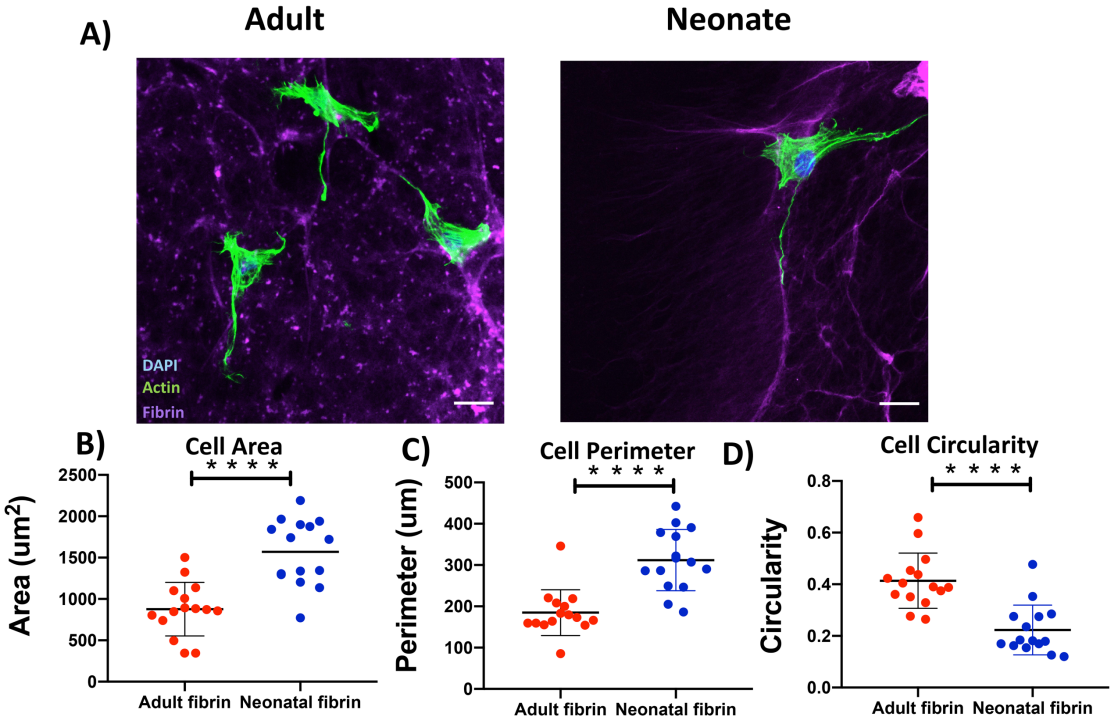

Figure 4. Fibroblast spreading is greater on neonatal fibrin films. (A) Representative confocal microscopy images of fibroblast morphology on neonatal or adult fibrin films at 40x. Cells were seeded on fluorescently labeled fibrin networks (purple) at a density of 6,000 cells per well for 16 hours prior to fixation. Fluorescent phalloidin (green) was used for membrane visualization. (B) Cell area, (C) perimeter, and (D) circularity was quantified with ImageJ. Mean +/- standard deviation is shown. Scale = 10 μm. p****<0.0001. N=15 cells per group.

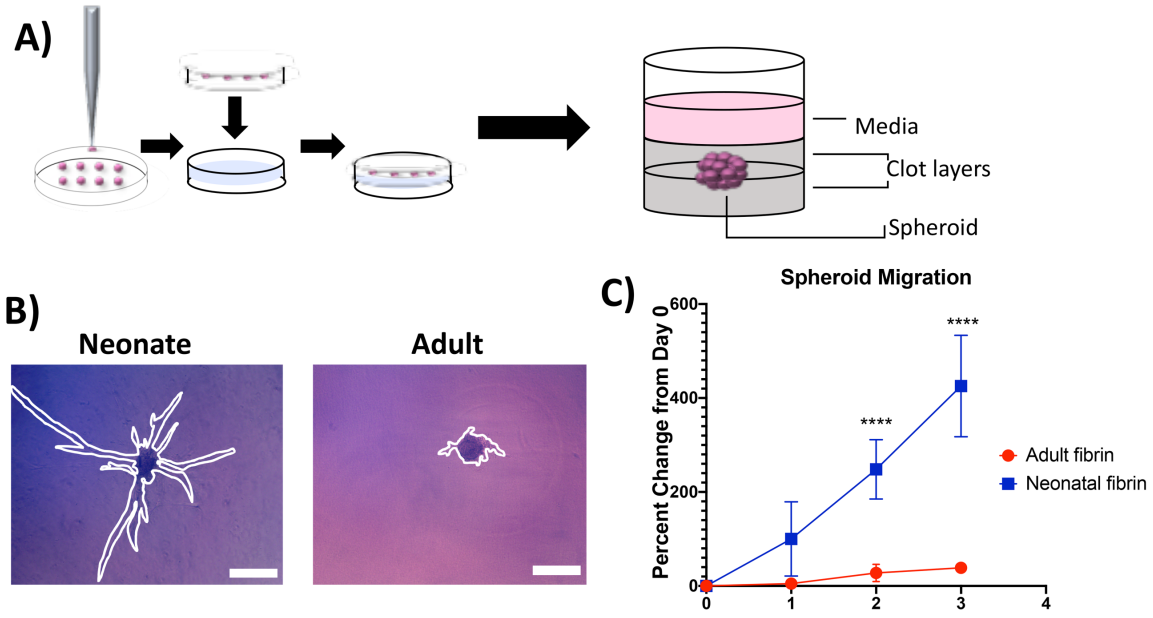

Figure 5. Fibroblast migration is accelerated through neonatal fibrin scaffolds compared to adult fibrin scaffolds. (A) Schematic of spheroid migration assay utilized to characterize fibroblast migration through 3D fibrin scaffolds. HDFns are cultured into spheroids and subsequently embedded in a 3D fibrin scaffold. Migration away from the spheroid body is measured daily for 72 hours and is quantified by measuring the spheroid boundary using Image J. (B) Representative images of cell migration outward from the spheroid after 72 hours imaged at 10x. Fibroblast outgrowth is outlined in white. (C) Migration results over 72 hours. Mean areas +/- standard deviation is shown. Scale = 200 μm. N=3-5/group. p***<0.001.

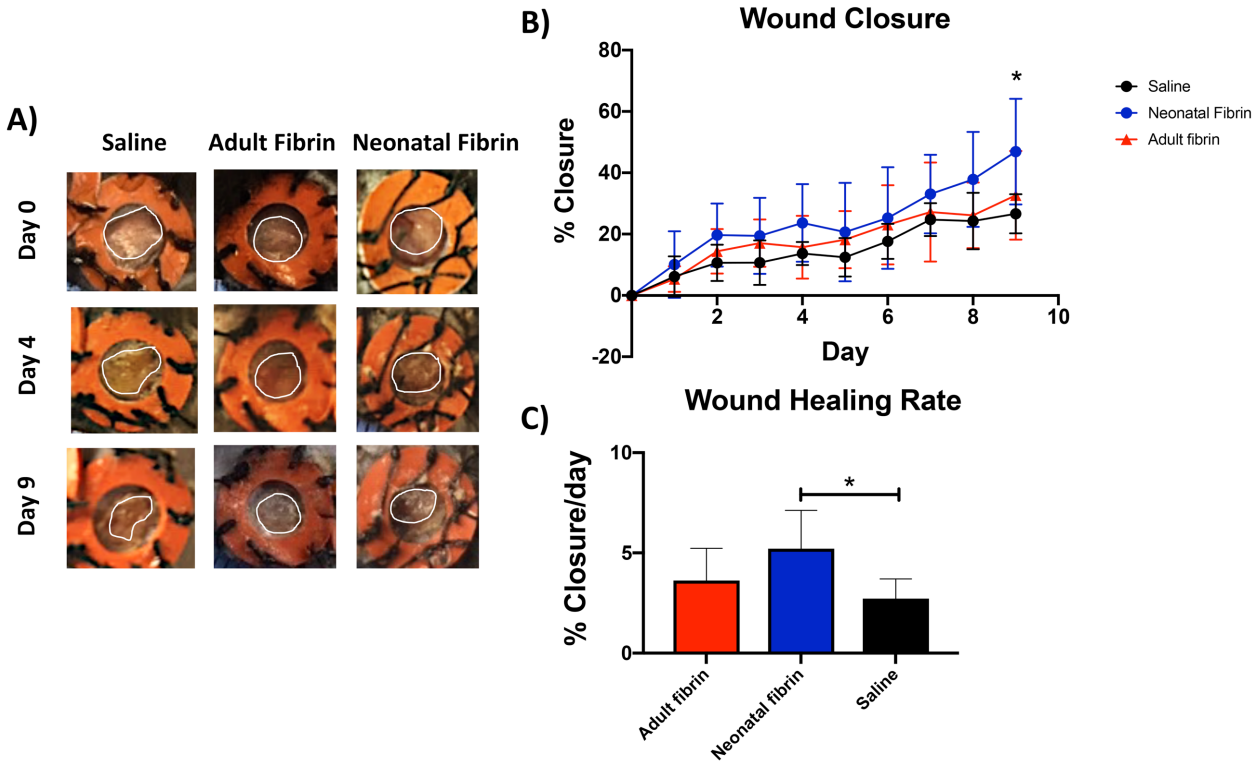

Figure 6. Wound closure is accelerated in the presence of neonatal fibrin scaffolds compared to adult fibrin scaffolds. (A) Neonatal or adult derived fibrin scaffolds were applied to a rodent full thickness dermal injury and wound healing was monitored over 9 days. Representative images of wounds treated with neonatal fibrin, adult fibrin, or saline on day 0, 4, and 9, (B) % wound closure over 9 days and (C) wound healing rate are shown. Means +/- standard deviation are shown. N=6 wounds per group. p*<0.05.

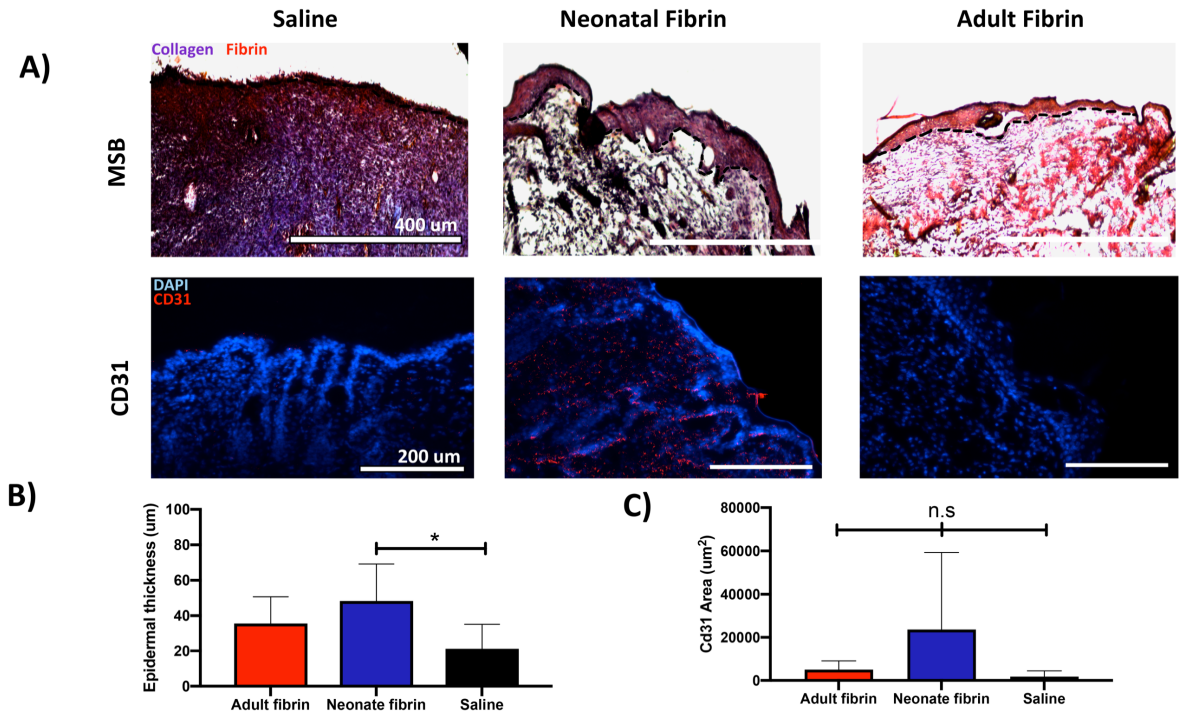

Figure 7. Neonatal fibrin scaffolds enhance epidermal thickness and angiogenesis compared to adult fibrin scaffolds. (A) Representative images of wounds stained with MSB and CD31 at 10x. (B) Quantification of images was performed by measuring thickness of epidermal layer in ImageJ and using ImageJ particle analysis to measure CD31 (red) area. MSB staining revealed significantly greater epidermal thickness in wounds treated with neonatal fibrin scaffolds. N=5-6. Immunolabeling for CD31+ tissue suggests enhanced, though not statistically significant, angiogenesis in wounds treated with neonatal fibrin. N=4-6. Means +/- standard deviation is shown. p*<0.05.

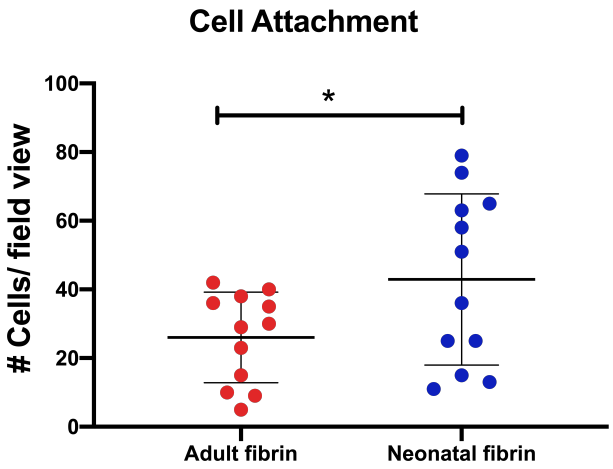

Supplemental Figure 1. Fibroblast attachment is greater on neonatal fibrin scaffolds. HDFns were seeded on neonatal or adult derived fibrin scaffolds at a density of 12,000 cells per well and incubated for 16 hours prior to fixation. Cells were labeled fluorescently labeled for visualization on confocal microscopy. Cell count was quantified as number of cells per viewing area. Mean cell count +/- standard deviation is shown. N=12 images per group. P*<0.05.

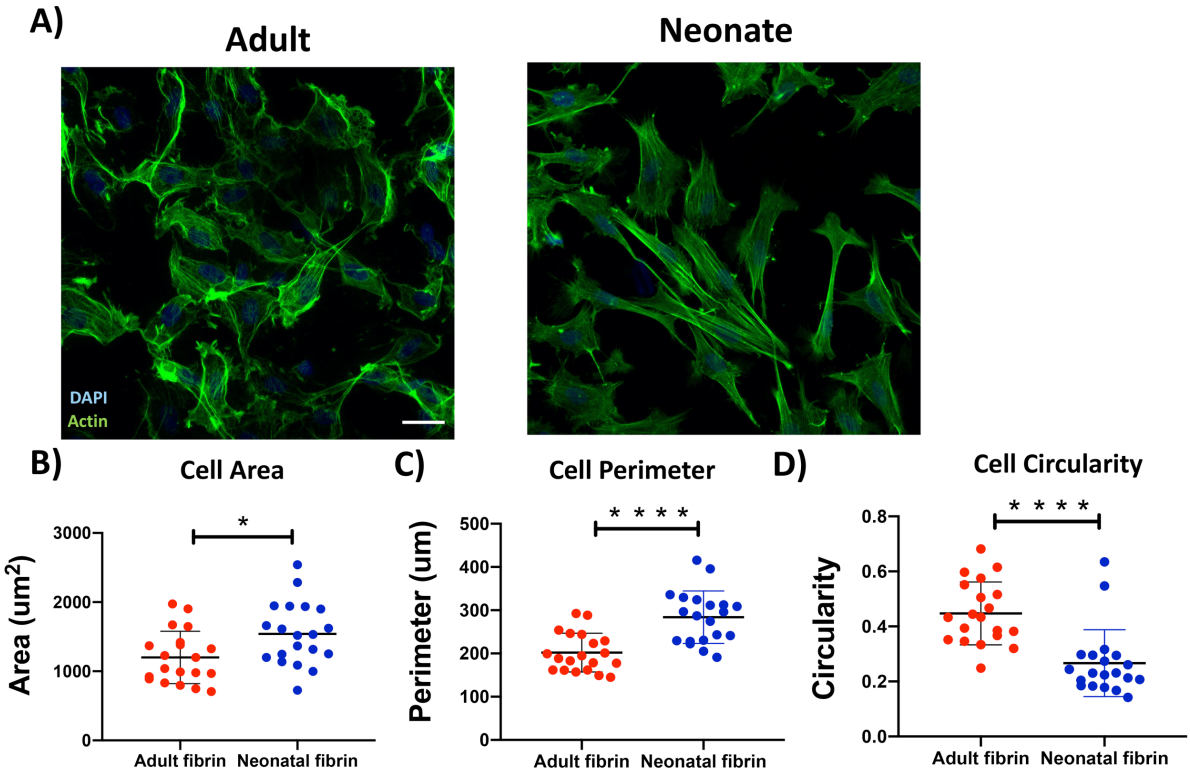

Supplemental Figure 2. Fibroblast spreading is greater on neonatal fibrin films. (A) Representative confocal microscopy images of fibroblast morphology on neonatal or adult fibrin films at 40x. Cells were seeded on fibrin networks at a density of 12,000 cells per well and incubated for 16 hours prior to fixation. Fluorescent phalloidin (green) was used for membrane visualization. (B) Cell area, (C) perimeter, and (D) circularity was quantified with ImageJ. Mean values +/- standard deviation are shown. N=20 cells per group. Scale = 10 μm. p*<0.05, p****<0.0001.